

A NOVEL AC VOLTAGE REGULATOR

Awad EL-SABBE and Ashraf ZEIN EL-DIN

Department of Electrical Engineering, Faculty of Engineering,

Menoufia University, Shebin El-kom, Egypt.

Tel.: XX(048) 221549, Fax.: XX(048) 235695, e-mail : IN % "et001@ shebin.eun.eg"

Abstract

This paper describes a new single phase regulator for supplying resistive loads, with two different strategies. Load voltage is varied by controlling the flux linkage of a single phase transformer windings used with the proposed system. The primary of the transformer is connected in series with the load to the ac supply, while the secondary is shunted with a control device. The flux linkage is controlled by using either a pair of thyristor "triac" (phase controlled) or a MOSFET transistor (ac chopper topology). Simulation analyses of the two proposed methods of control are presented, and verified by experimental results in different cases of operation. The advantages of a proposed system are simple, effective, accurate, low distortion of supply current, smooth regulation of load voltage and low cost. The proposed system can be used in industry applications such as heaters, lighting control and ac drives controls.

Keywords

Ac voltage regulators, triac, thyristor controllers, MOSFET, magnetic circuit and microprocessor.

1. Introduction

Ac voltage regulator have been widely used to obtain variable ac voltage from a fixed ac source. The phase angle control of ac voltage regulator is extensively employed in many applications such as industrial heating, lighting control and speed control of ac drives. This technique offers the advantages of simplicity and ability of controlling large amount of power economically. The conventional ac voltage regulators suffer from the higher harmonic content in the supply current and low power factor particularly at delayed firing angles. These problems can be solved by using harmonic filters, but that is not suitable for all control range [1] using different construction of controller, however the operation is complicated. Modification of the power circuit such as controlling of flux or inductance of magnetic circuit can be used in the controller circuit. The moving coil regulators[2], provide smooth voltage regulation at the output terminals without any distortion (pure sinusoidal waveform). However, this regulator is complex and costly. Variable inductors such as variable air-gap type inductor and tap changing inductor can be smoothly varied to control the load voltage [3]. However, these devices suffer from certain drawbacks, such as necessity of mechanical operation, slow time response and complexity of operation. In most cases, the improvement of supply current wave form is not noticeably.

In development of power semiconductor devices, Pulse Width Modulation (PWM), ac voltage chopper technique is used. The output voltage of ac chopper can be changes from zero to 100% , of the supply voltage by varying the ON/OFF time ratios of a series controlled switch. Using a microprocessor as a controller makes it possible to vary the

Manuscript received from Dr: Awad El- Sabbe at: 10/ 6/ 1997,

Accepted at: 20/ 7/ 1997, pp. 1-20,

Engineering research bulletin, Vol. 20, No. 3, 1997,

Menoufiya University, Faculty of Engineering,

Shebin El-Kom, Egypt, ISSN. 1110-1180.

ON/OFF ratio according to a predetermined timing region [4], [5]. However, the power factor at the supply terminals, is hard to control and may be improved indirectly. Using a single phase transformer with a single controlled device will controlling the output voltage and frequencies, when an integral control technique is applied. However, the input power factor is poor, more distortion in the supply current and effect of voltage flickers is not easily avoided [6], [7] and [8].

A simplified ac voltage controller is presented in this paper. Two different strategies are proposed to control the load voltage namely; phase angle control using a pair of thyristor or triac and an ac voltage chopper using only one MOSFET transistor. Applying such techniques with the proposed chopper controller will reduce the supply harmonics content and improve its power factor. The result has been obtained by solving the equations using numerical techniques and comparison between the two proposed strategies are presented

2. System description, analysis and results of the first proposal

With respect to Fig.1, the proposed circuit of the first technique consists of a pair of thyristor (triac), shunted with the secondary windings of a single phase transformer having a transformation ratio equals one. The primary windings of the transformer are connected in series with the load across the ac supply. Conventional firing circuit is employed, a firing pluses is produced every half cycle of the supply frequency. The firing pluses are phase controlled with respect to the supply voltage .

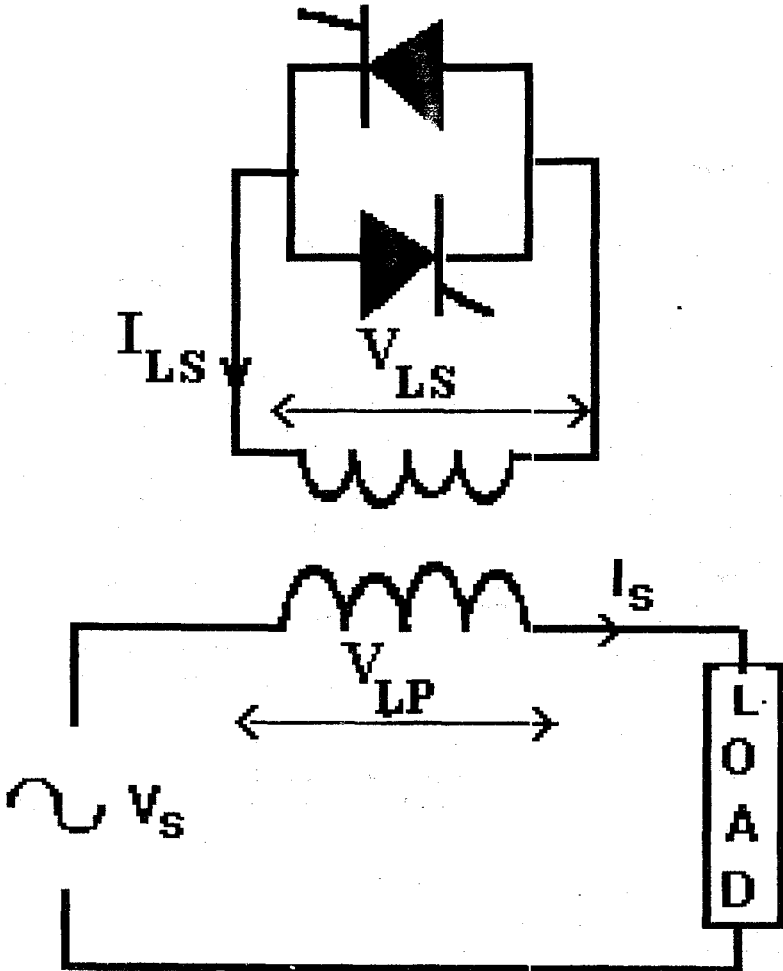


Fig. 1 Schematic diagram of first proposed system

When the triac is in mode off, load current flows causing flux linkage with the transformer secondary winding (λ_{21}), and induced voltage at the secondary terminals (V_{1s}). The transformer can be considered as an equivalent inductance connected in series with the load. At firing angle (α) the triac turns ON shorting the secondary; the mutual flux linkage ($\lambda_{12} = \lambda_{21}$) between primary and secondary windings will decay as the secondary current decay. When the stored energy in the magnetic field discharged the triac naturally turned OFF.

The system equations when the thyristor OFF are :

$$V_s = i_s R_L + i_s R_p + L_p \frac{di_s}{dt} + \frac{d\lambda_{12}}{dt} \quad (1)$$

$$V_{Ls} = \frac{d\lambda_{21}}{dt} \quad (2)$$

On the other hand as the triac fired (thyristor ON) at $wt = \alpha$, the system equations are :

$$V_s = i_s R_L + i_s R_p + L_p \frac{di_s}{dt} + \frac{d\lambda_{12}}{dt} \quad (3)$$

$$V_{Ls} = i_{Ls} R_s + L_s \frac{di_{Ls}}{dt} + \frac{d\lambda_{21}}{dt} = 0 \quad (4)$$

A computer program has been constructed for solving equations 1, 2, 3 and 4 using the 4th order Runge-Kutta of numerical method with a step of 100 μ sec. Samples of theoretical and experimental results with a load resistance of 47 ohm and 110 volt ac supply, are shown in Figs. 2 and 3 at firing angles 30° and 90° . It can be seen that, the comparison reveals a good agreement between theoretical and experimental waveforms. Also, by controlling the firing angle of triac, load voltage is varied easily. As the R-load is replaced by R-L load, Figs. 4, 5 and 6 show the experimental results of terminal voltage, load current, primary and secondary coil terminal voltages at variation of load inductance between minimum value (102 m.H.) to maximum value 0.95 H at 90° firing angle. This results indicate clearly that the variation of load voltage affects the primary and secondary coil terminal voltages, the spice of voltage increases as the increasing of load inductance. We replace a dynamic load (single phase induction motor 1420 r.p.m., 220 volt., 0.5 HP) instead of the pervious R-L load, the experiment results in Fig. 7 shows motor terminal voltage and current at firing angle equals to 90° , also primary and secondary coil terminal voltages. We obtain a good results at dynamic load as the same the pervious results.

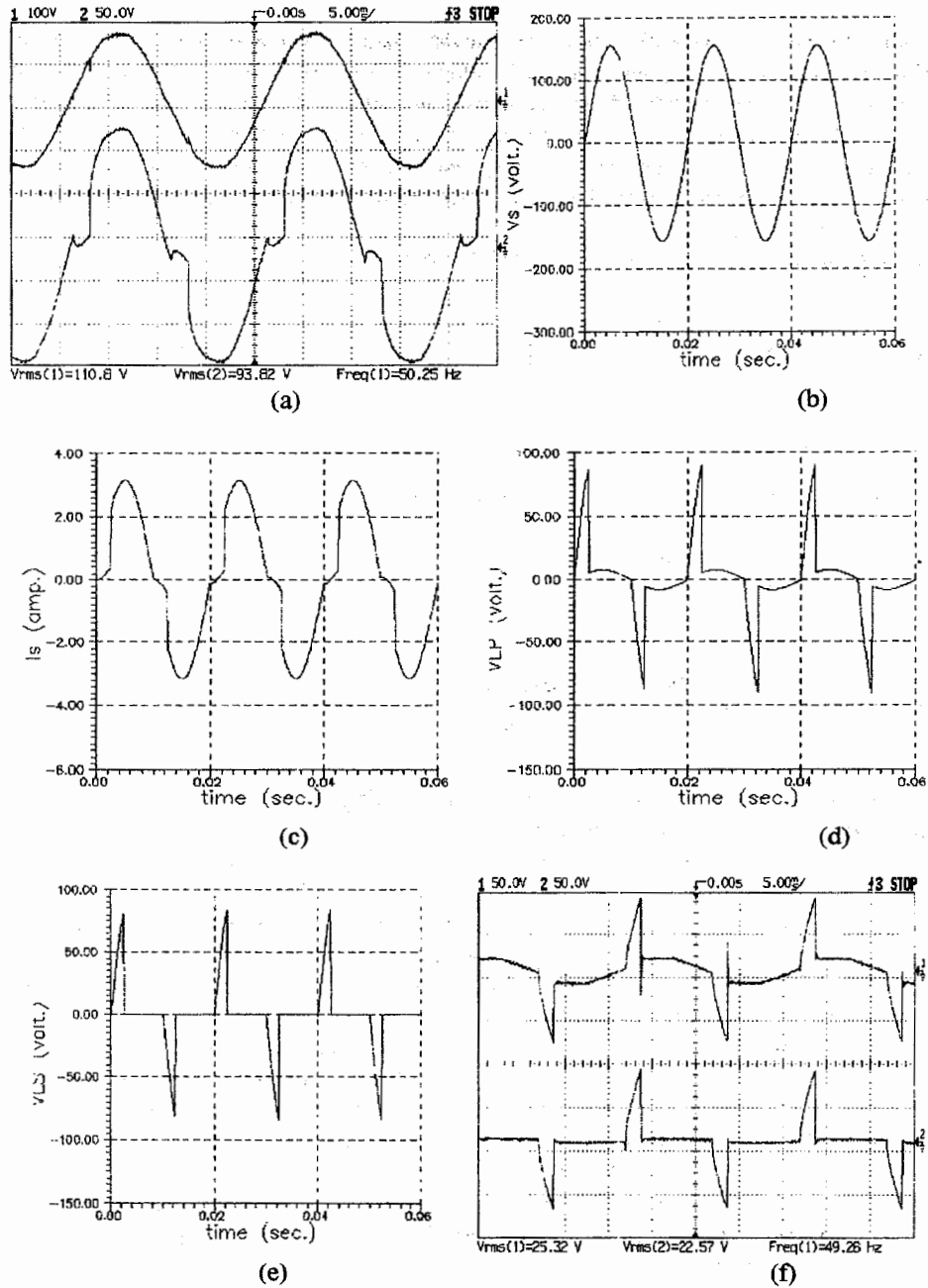


Fig. 2 Experimental and theoretical results for $\alpha = 30^\circ$. (a) Experimental supply voltage and current. (b) Simulation supply voltage. (c) Simulation supply current. (d) Simulation primary terminal voltage. (e) Simulation secondary terminal voltage. (f) Experimental primary and secondary terminal voltage

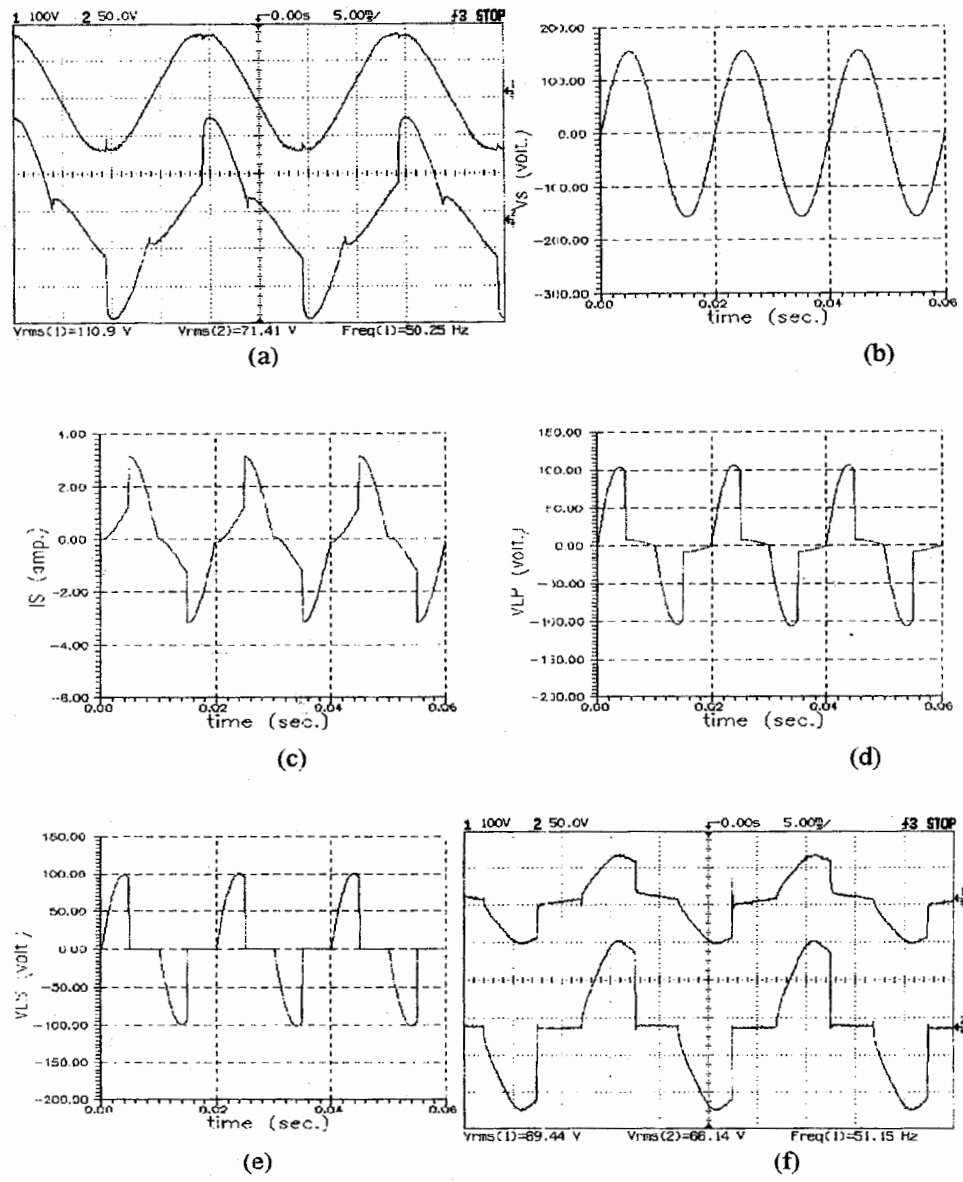
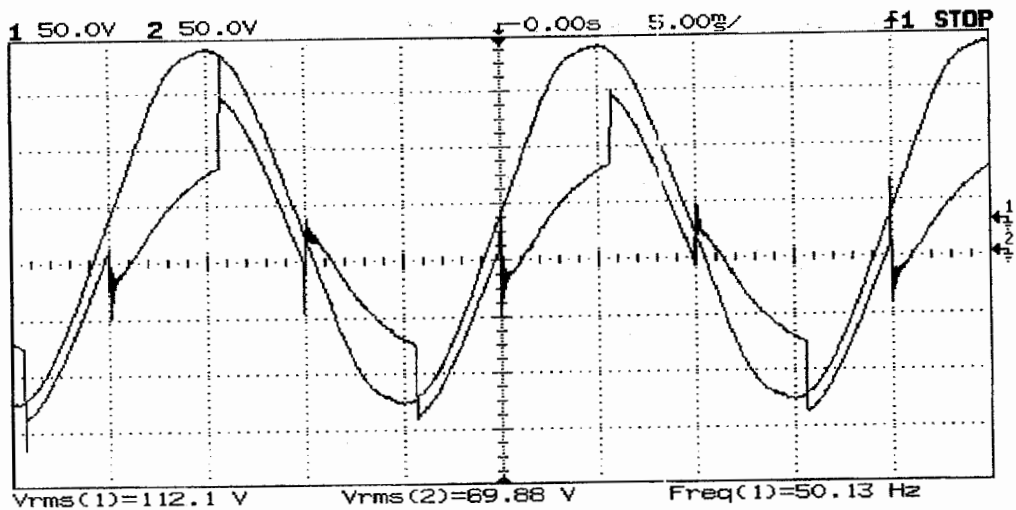
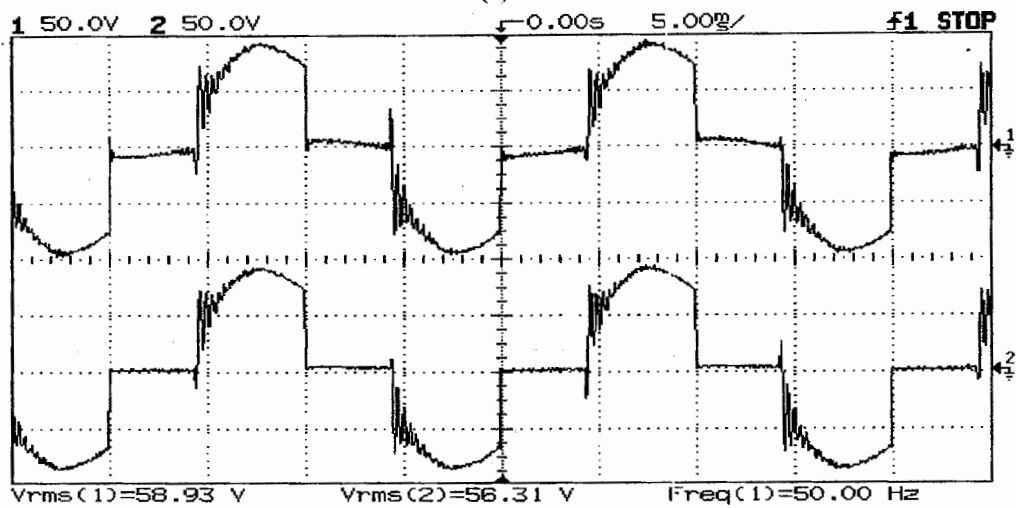


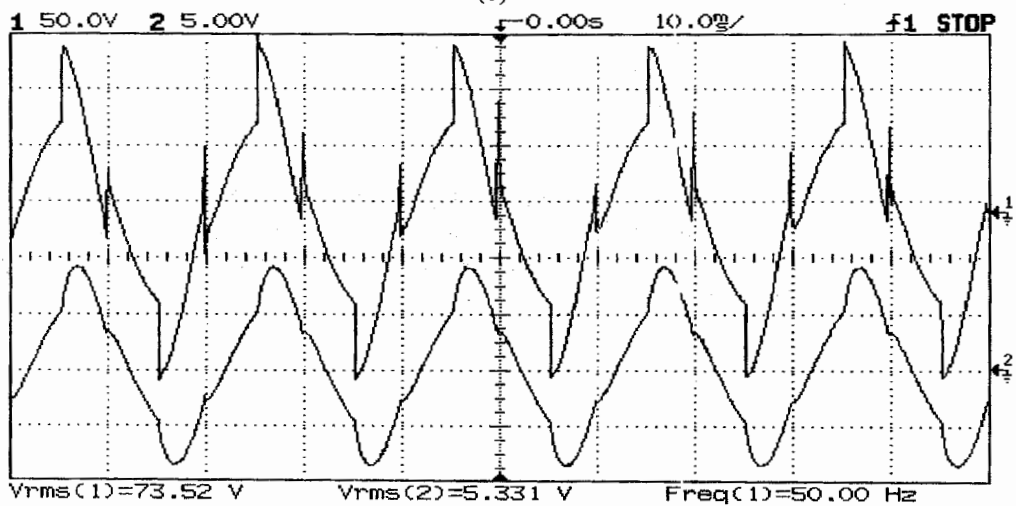
Fig. 3 Experimental and theoretical results for $\alpha = 90^\circ$. (a) Experimental supply voltage and current. (b) Simulation supply voltage. (c) Simulation supply current. (d) Simulation primary terminal voltage. (e) Simulation secondary terminal voltage. (f) Experimental primary and secondary terminal voltage



(a)



(b)



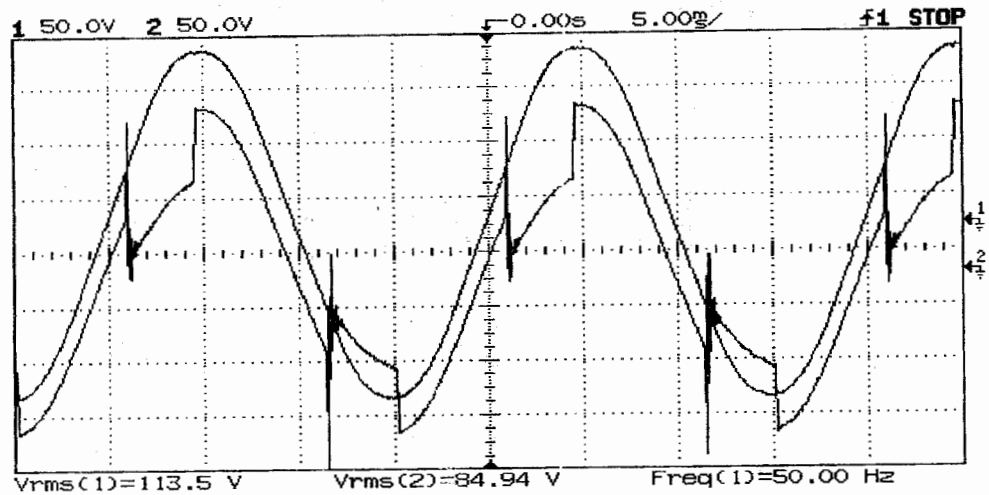
(c)

Fig. 4 Experimental results at $\alpha = 90^\circ$, R-L load ($R= 50$ ohm, and $L= 102$ m.H.).

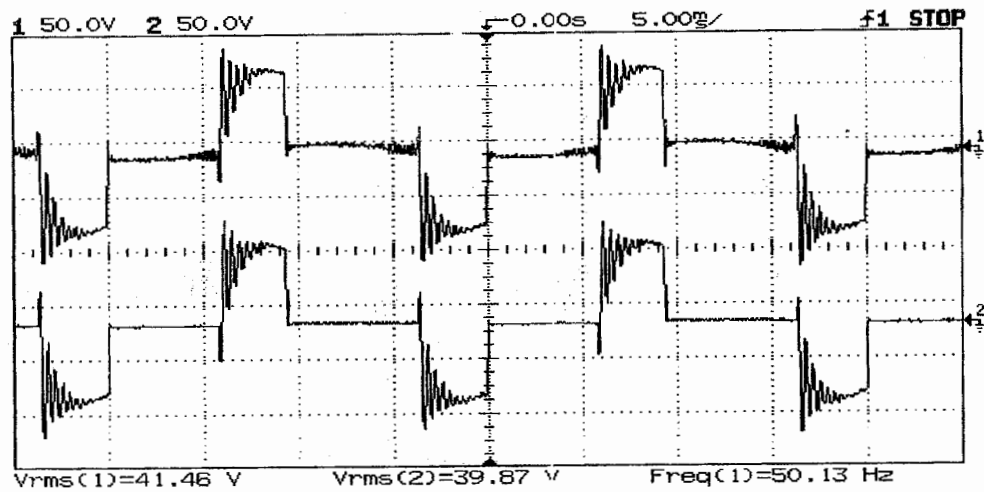
(a) Supply voltage and Load voltage .

(b) primary and secondary terminal voltage

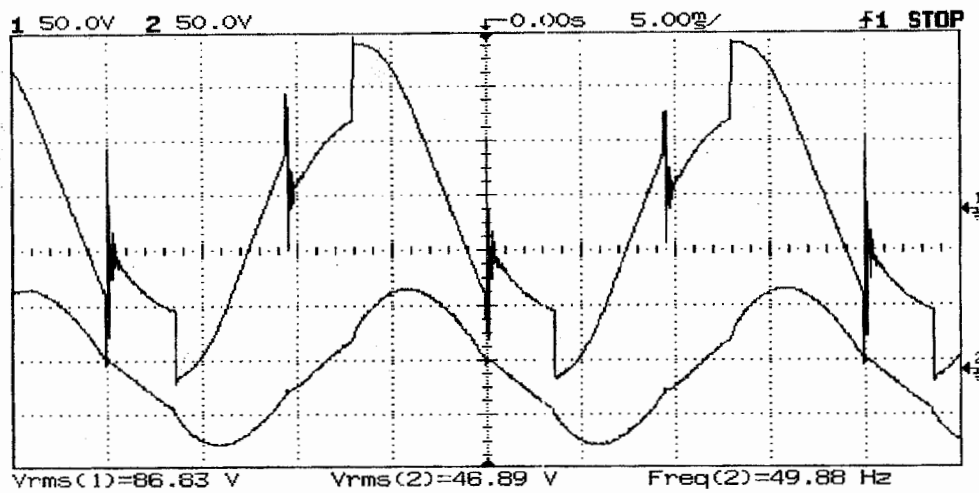
(c) Load voltage and current



(a)



(b)



(c)

Fig. 5 Experimental results at $\alpha = 90^\circ$, R-L load ($R = 50 \text{ ohm}$, and $L = 199 \text{ m.H.}$).
 (a) Supply voltage and Load voltage .
 (b) primary and secondary terminal voltage
 (c) Load voltage and current

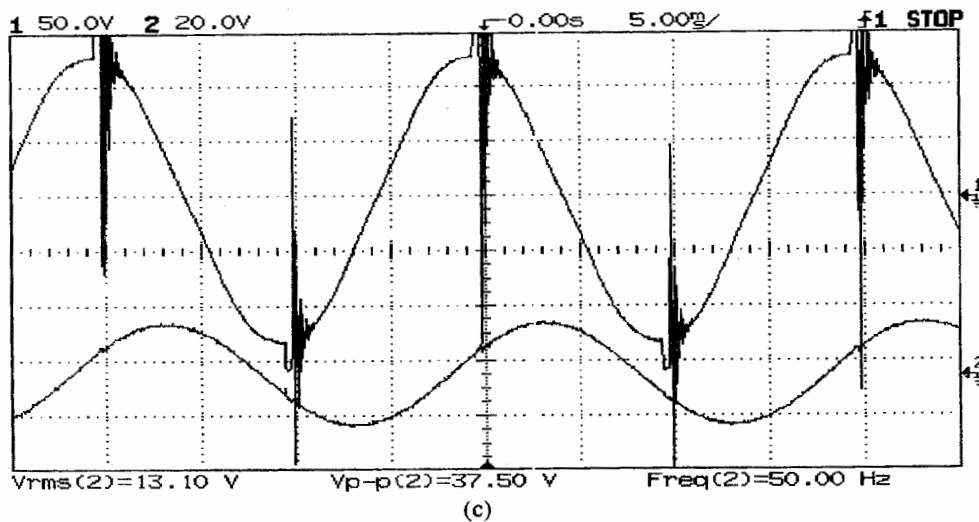
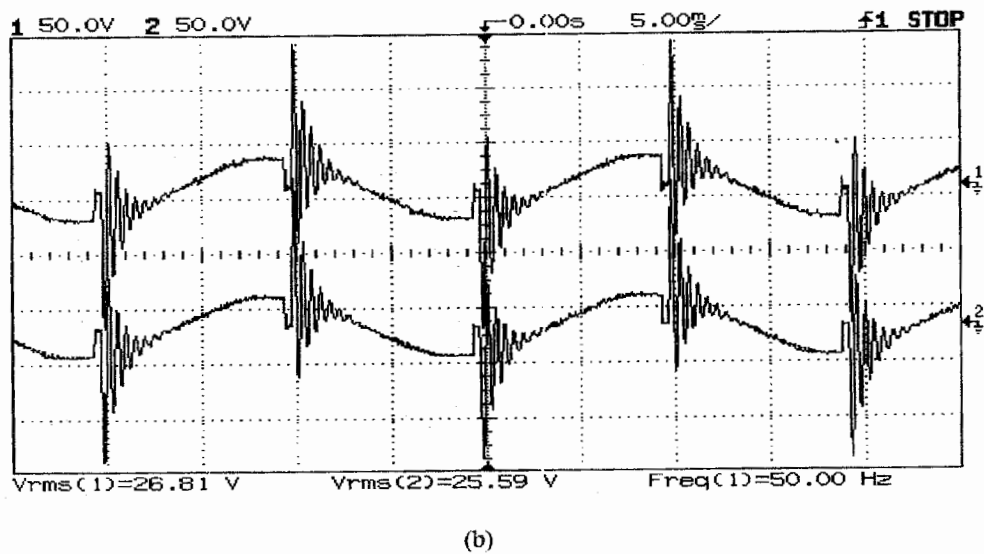
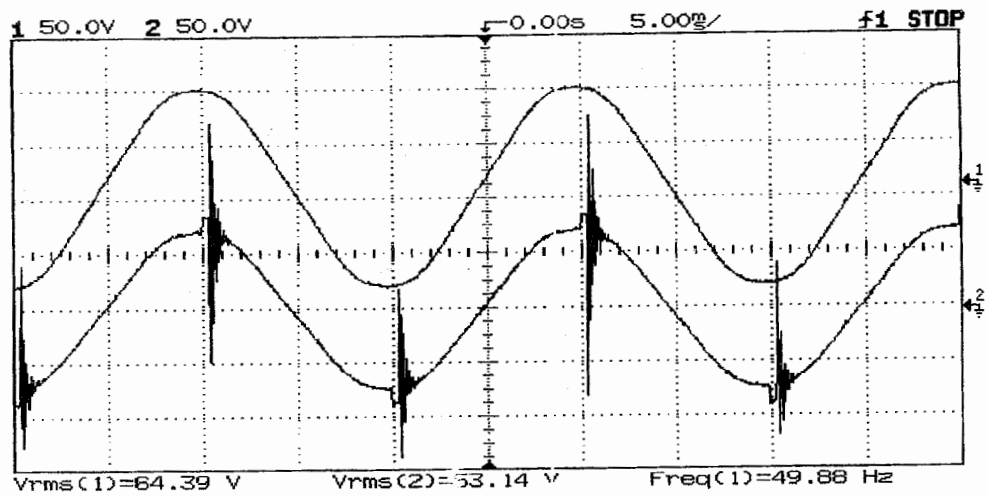
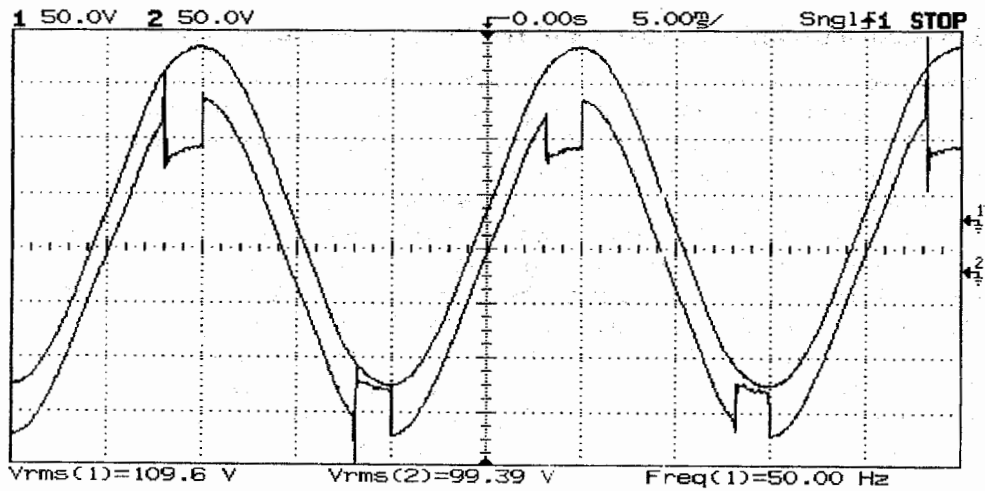
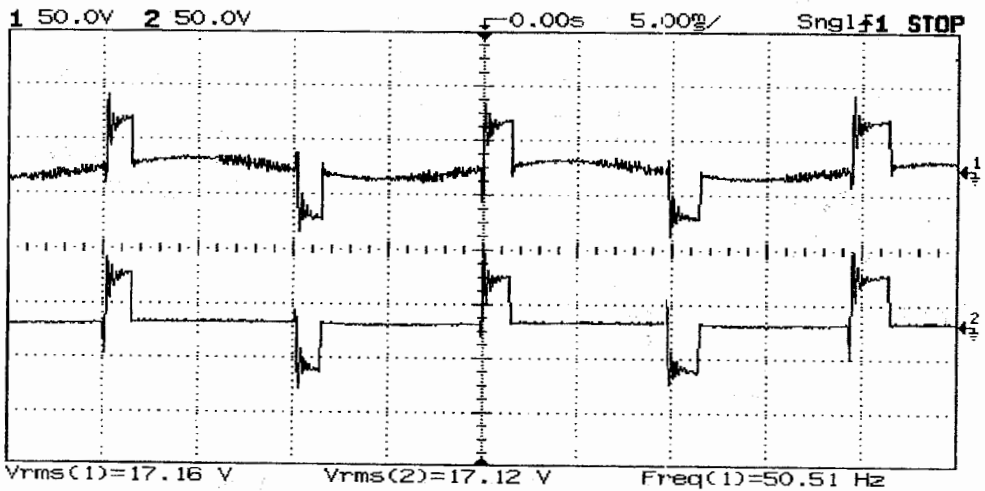


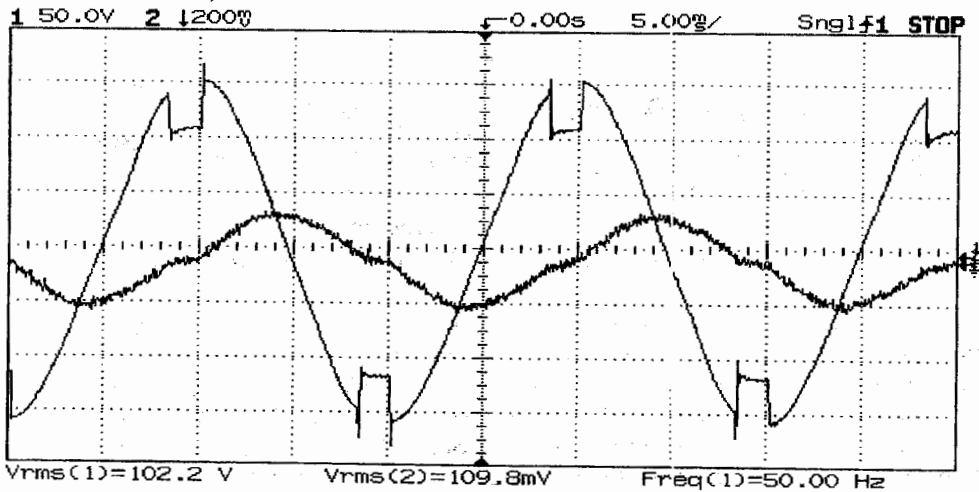
Fig. 6 Experimental results at $\alpha = 90^\circ$, R-L load ($R=50$ ohm, and $L=950$ m.H.).
 (a) Supply voltage and Load voltage .
 (b) primary and secondary terminal voltage
 (c) Load voltage and current



(a)



(b)



(c)

Fig. 6 Experimental results of single phase induction motor at $\alpha = 90^\circ$,
 (a) Supply voltage and Load voltage .
 (b) primary and secondary terminal voltage
 (c) Load voltage and current

3. System description, analysis and results of the second proposal

With respect to Figs. 8-a, b, c and d, the transformer secondary terminals is connected through a diode bridge rectifier to a dc chopper switch, this switch is a power transistor (MOSFET). Turn on (T_{on}) or turn off (T_{off}) of the transistor is achieved through its driver circuit which situated between it and a microprocessor. Square wave signal (synchronization signal) delivers through input port of microprocessor corresponds to input a-c supply voltage. The required number of pulses for MOSFET are stored in memory locations depending upon mark/space ratio. The MOSFET can be operate at a given mark/space ratio determined from the microprocessor in order to control the load voltage. Equations 1 and 2 can be applied when the MOSFET is OFF, but equations 3 and 4 can be used when the MOSFET is ON. An assembly program is written to vary the mark/space ratio between 0 to 1 and the output pulses from output ports of the microprocessor are used to control MOSFET operation either ON or OFF according to a desired load voltage. General flow chart of the control process is shown in Fig.8d

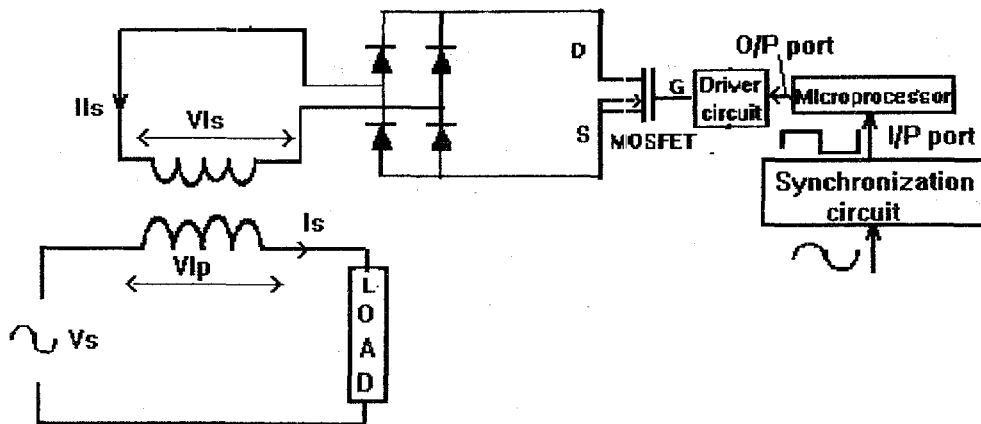


Fig. 8a Schematic diagram of second proposed system

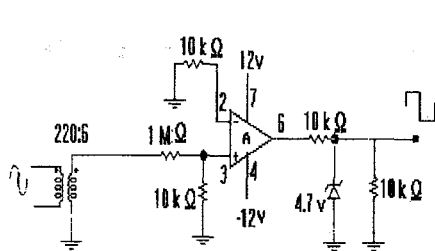


Fig.8b Synchronization circuit

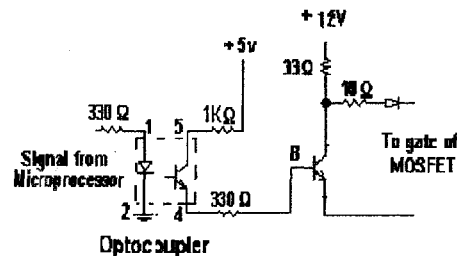


Fig. 8c MOSFET driver circuit

Samples of theoretical and experimental results of the second proposed system at different duty cycle are shown in Figs. 9, 10 and 11. In order to verify the second proposal system in case of R-L load ($R=50\text{ ohm}$ and $L=199\text{ mH}$) and dynamic load (universal motor 0.5 HP, 1 amp., 220 volt.) instead of R-load, as shown in Figs. 12, 13 and 14. The spikes appears in the experimental results are due to switching ON and OFF of the Mosfet and can be eliminated by using capacitor with suitable value at the load terminals or using a zener diode across the MOSFET terminals. From these Figures, It can be noticed that, as duty cycle is increased, spikes in supply voltage is decreased. Hence, by controlling mark/space ratio, load voltage is controlled easily and simple. Also, It can be seen that, the comparison between experimental and simulated results gives a good agreement.

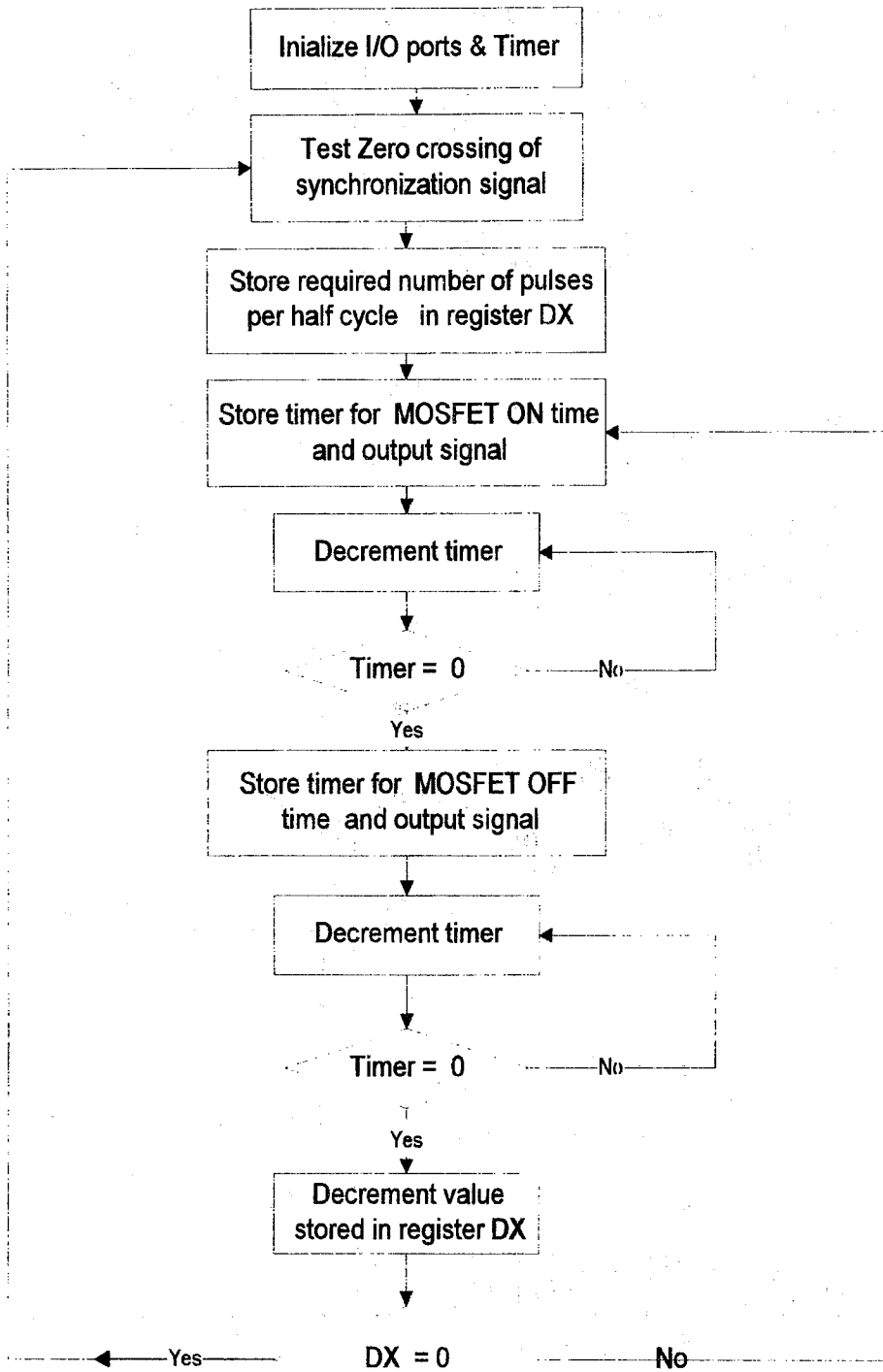


Fig.8d General flow chart of the control process

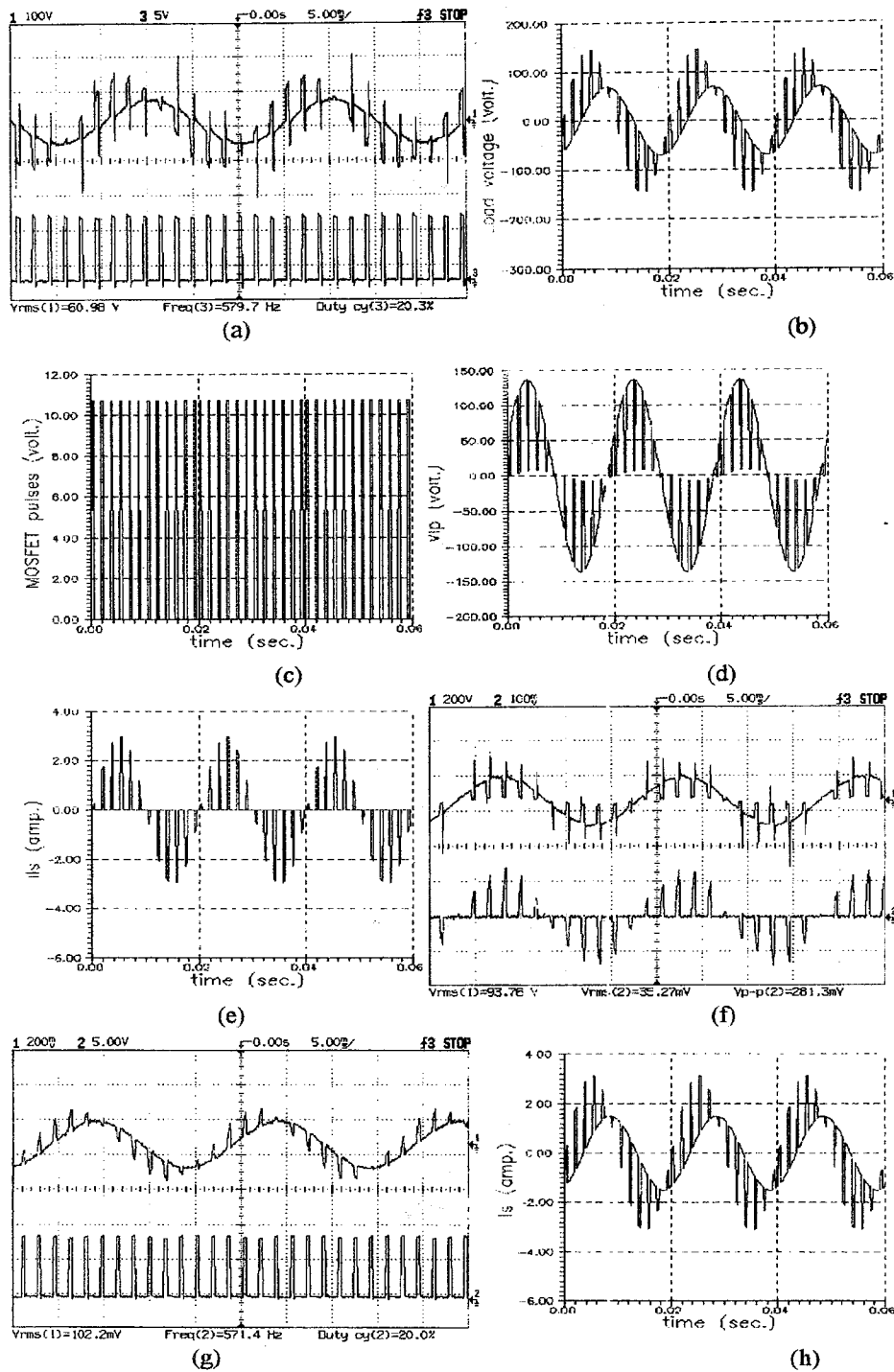


Fig. 9 Experimental and theoretical results for duty cycle=20.3% and MOSFET pulses frequency=579.7 Hz.

(a) Experimental supply voltage and MOSFET pulses. (b) Simulation supply voltage. (c) Simulation of MOSFET pulses (d) Simulation primary terminal voltage of transformer (e) Simulation secondary current of transformer (f) Experimental of primary winding terminal voltage and secondary current of transformer. (g) Experimental supply current and MOSFET pulses. (h) Simulation supply current.

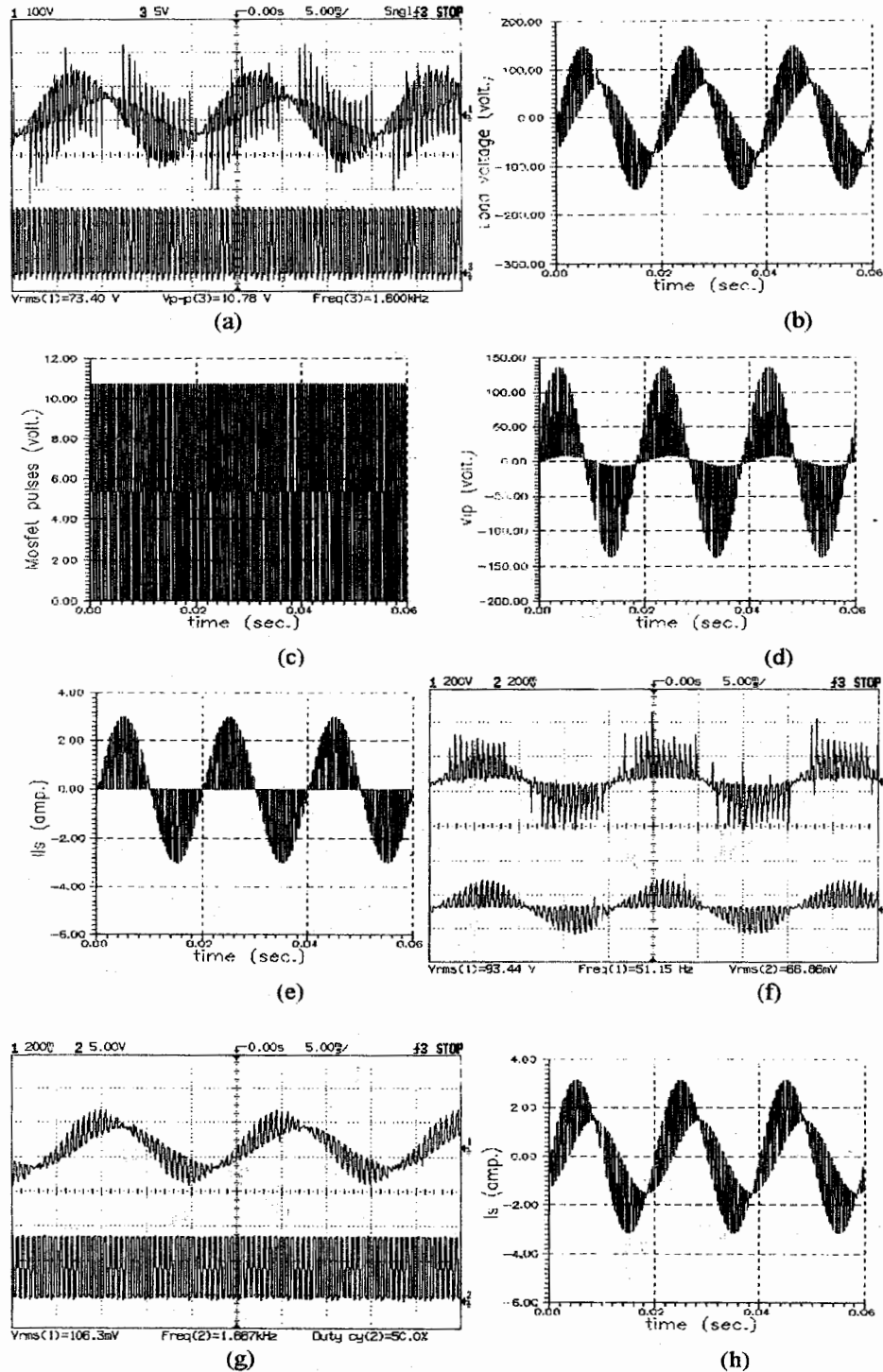


Fig. 10 Experimental and theoretical results for duty cycle=50 % and MOSFET pulses frequency=1.6 KHz .

- (a) Experimental supply voltage and MOSFET pulses. (b) Simulation supply voltage.
(c) Simulation of MOSFET pulses (d) Simulation primary terminal voltage of transformer
(e) Simulation secondary current of transformer (f) Experimental of primary winding terminal voltage and secondary current of transformer. (g) Experimental supply current and MOSFET pulses. (h) Simulation supply current.

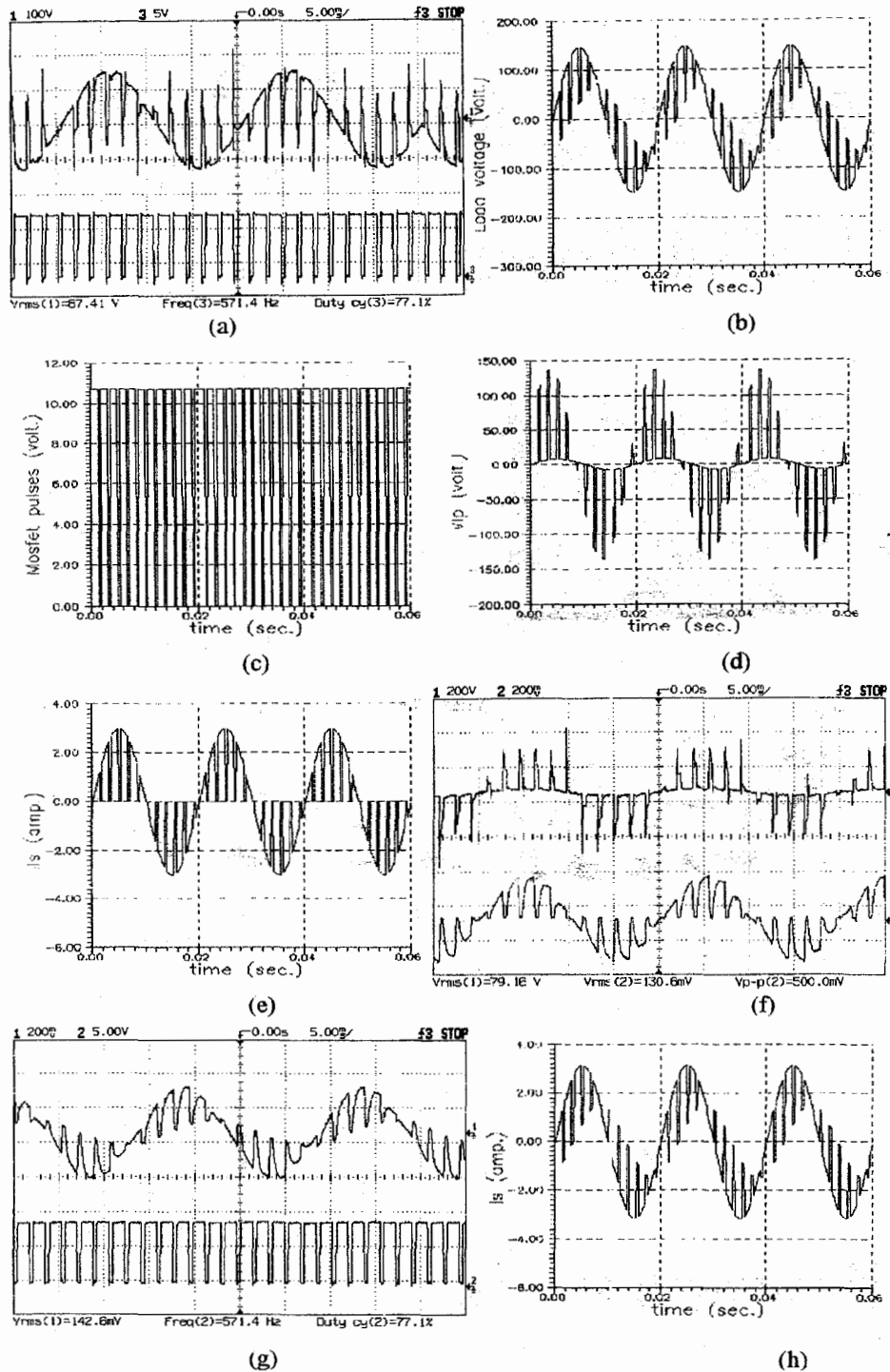
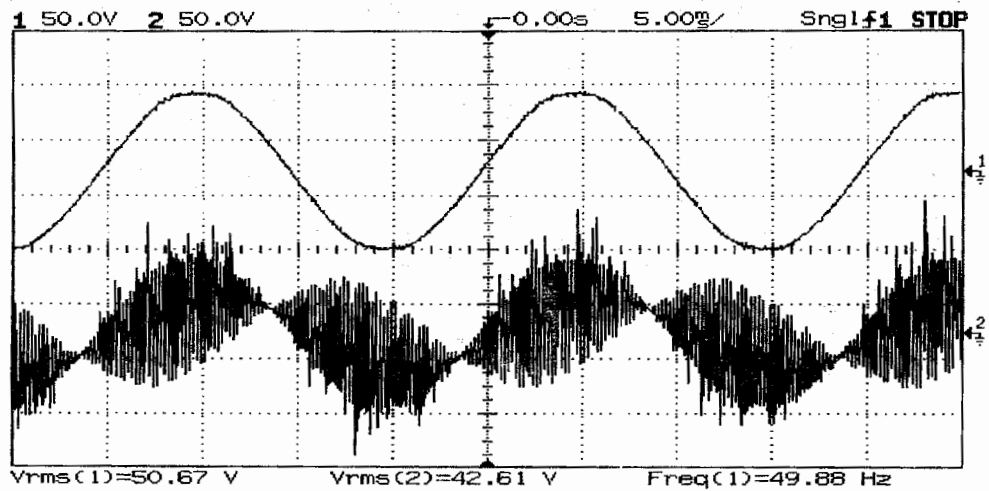
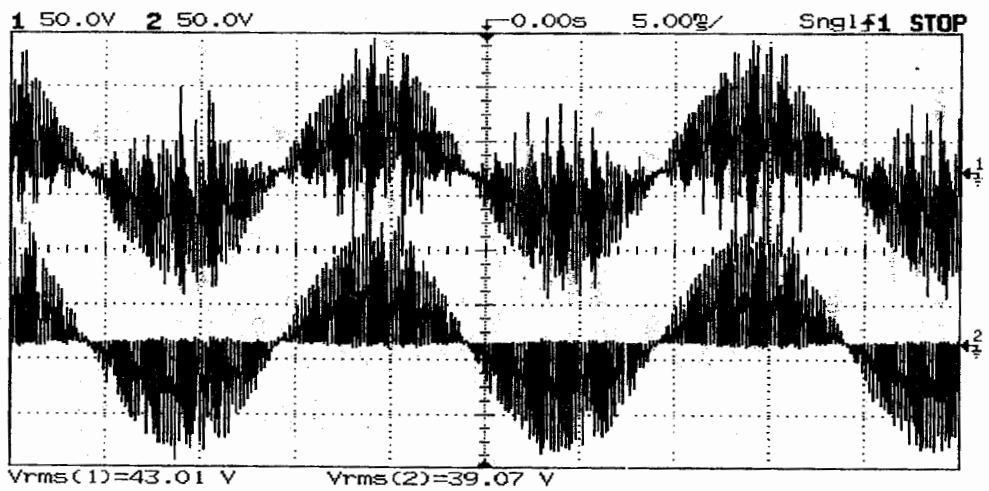


Fig. 11 Experimental and theoretical results for duty cycle=77.1 % and MOSFET pulses frequency=571.4 KHz .

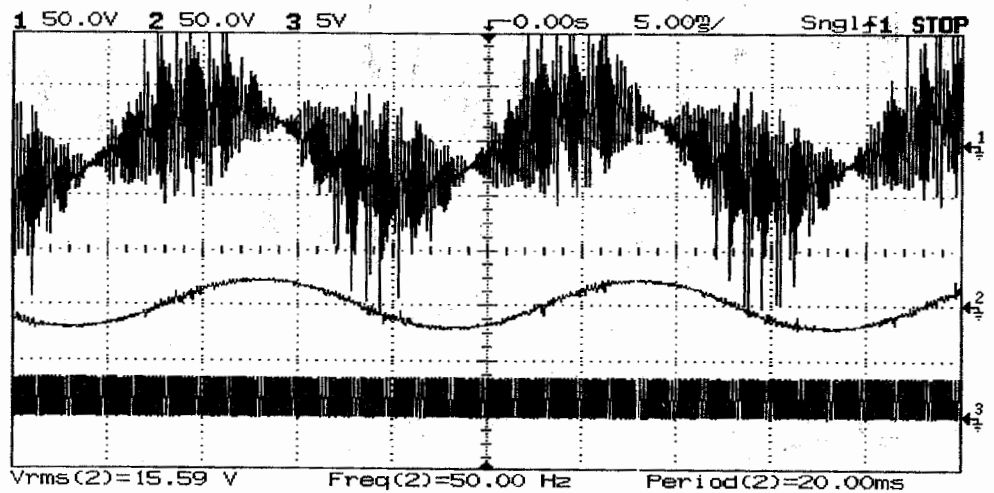
- (a) Experimental supply voltage and MOSFET pulses. (b) Simulation supply voltage. (c) Simulation of MOSFET pulses (d) Simulation primary terminal voltage of transformer (e) Simulation secondary current of transformer (f) Experimental of primary winding terminal voltage and secondary current of transformer. (g) Experimental supply current and MOSFET pulses. (h) Simulation supply current.



(a)



(b)



(c)

Fig. 12 Experimental results for duty cycle=50 % and MOSFET pulses frequency = 1.6 KHz (R-L load)
 (a) Supply voltage and Load voltage. (b) Primary terminal voltage of transformer
 (c) Load voltage, load current and MOSFET pulses .

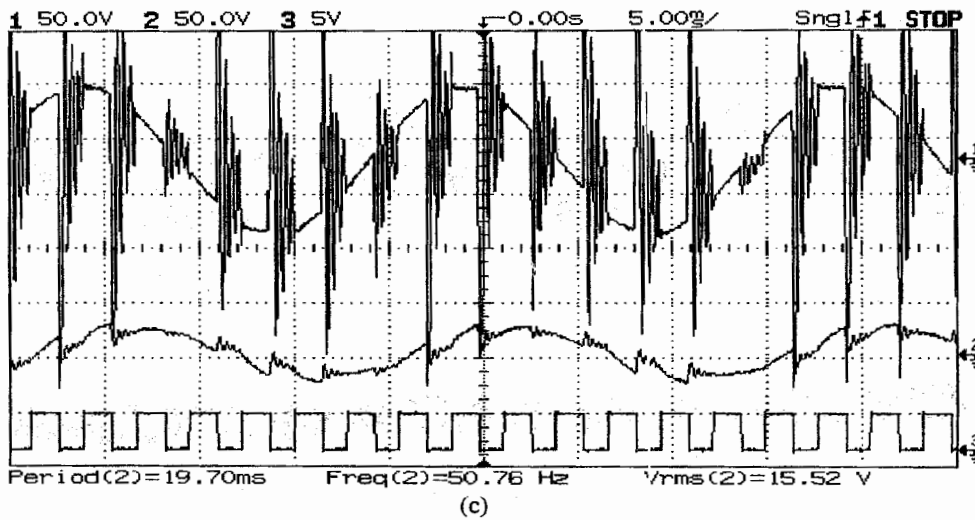
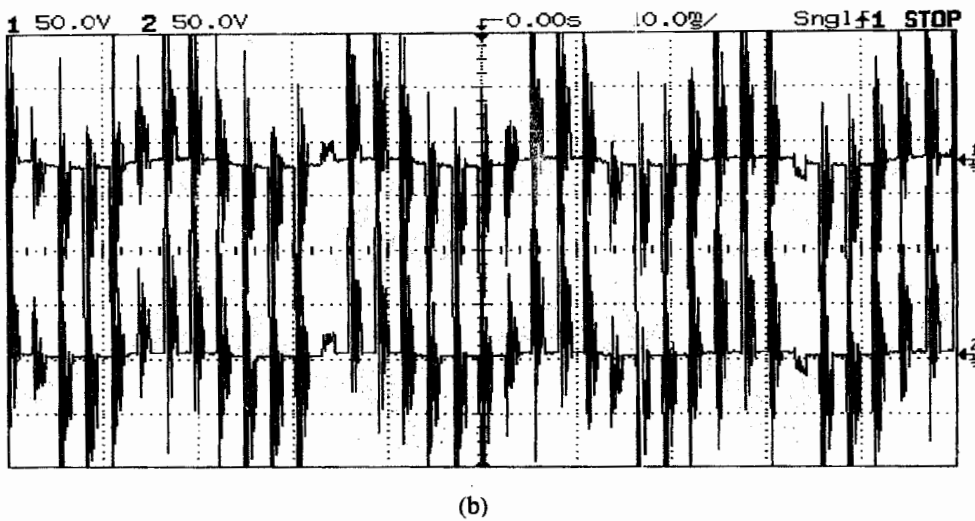
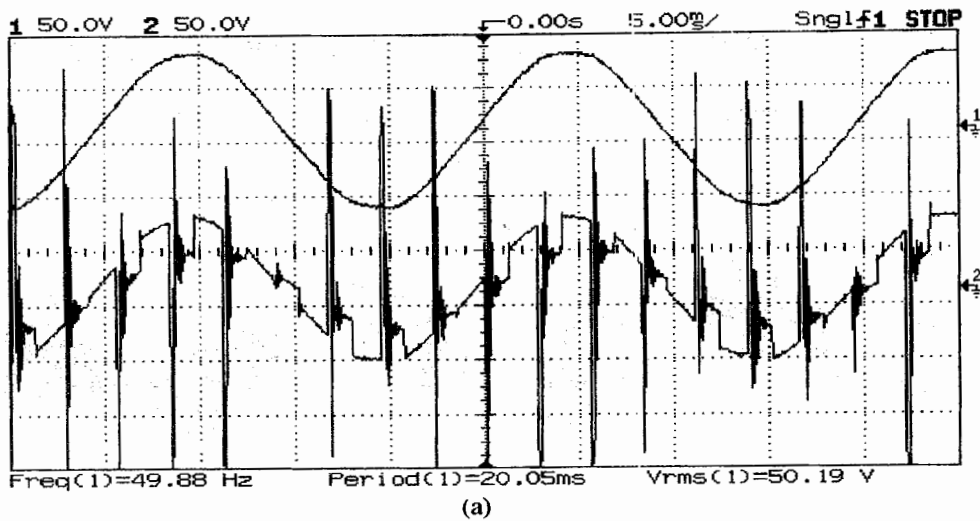


Fig. 13 Experimental results for duty cycle= 50 % and MOSFET pulses 400 Hz (R-L load)
 (a) Supply voltage and Load voltage. (b) Primary terminal voltage of transformer
 (c) Load voltage, load current and MOSFET pulses .

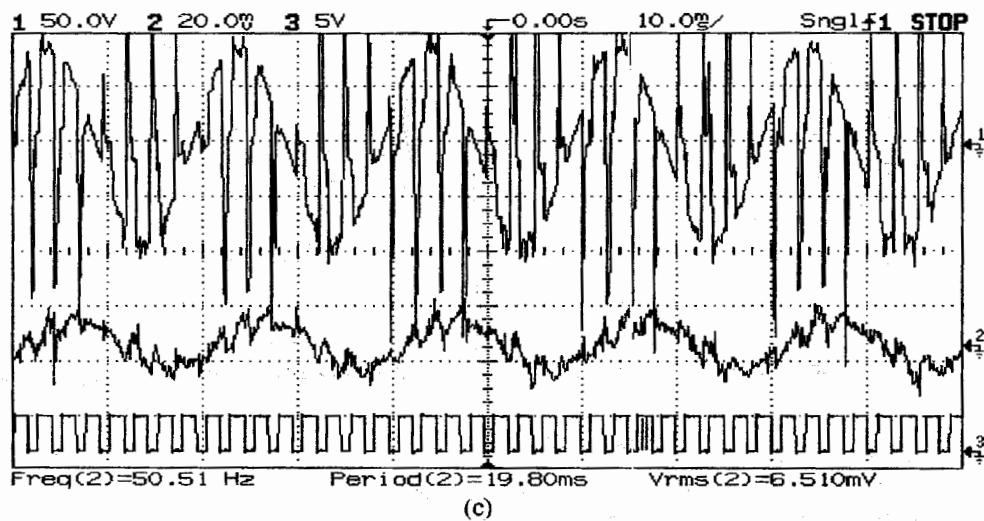
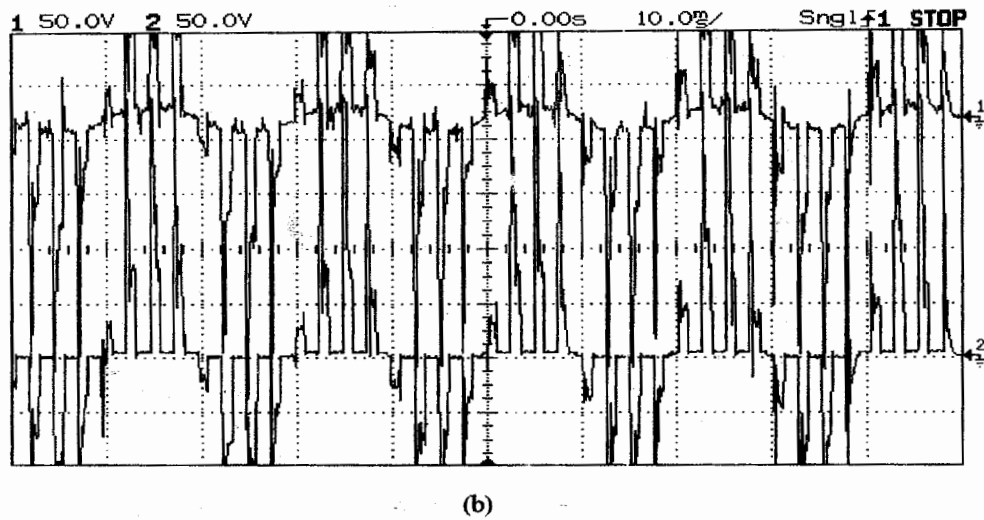
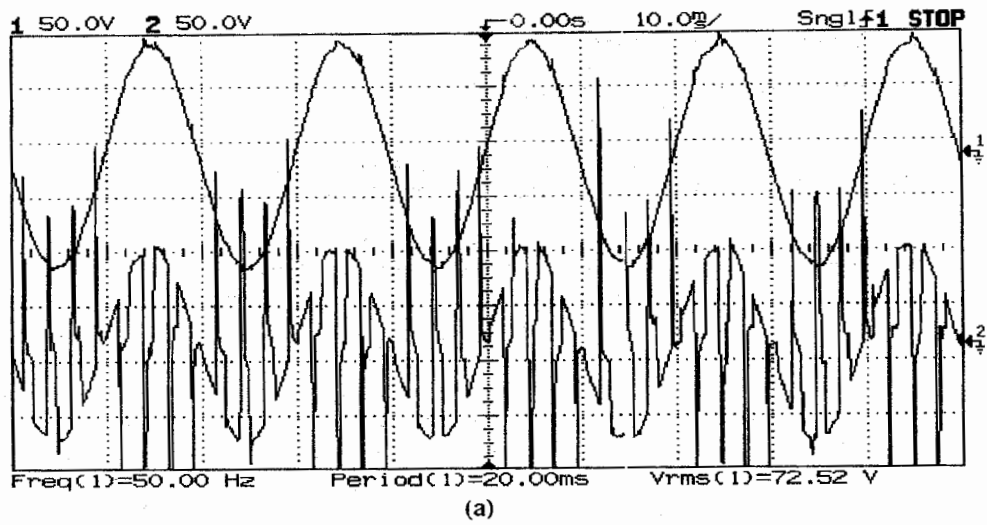


Fig. 14 Experimental results for dynamic load (universal motor)
 (a) Supply voltage and Load voltage. (b) Primary terminal voltage of transformer
 (c) Load voltage, load current and MOSFET pulses.

4. Power factor and harmonics

The power factor at supply terminals usually determined by :

$$\text{Power Factor} = \frac{\text{Active power at supply terminals}}{\text{total volt ampers at the supply terminals}}$$

Numerical techniques are used to solve the equations describes each system ,calculate the power, power factor and the harmonics spectrum at the supply terminals. Figure 15 shows the variation of power factor with the firing angle of thyristor ,where Fig 16, shows the harmonic spectrum of the supply current in the first system . The result shows that , the power factor is varied between 50% and 100% depending upon the control range . Also, a continuity of the supply current reduced the harmonic components at the supply terminals. For the second system, Figure 17, shows the variation of the power factor with the duty cycle. Figure 18 shows the spectrum of the the harmonic components at the supply terminals. In these curves it may be noticed that as the duty cycle increased the power factor at the supply is also increased. Also, increasing the duty cycle will decrease the harmonic components at the supply terminals where the supply current continuity increases with duty cycle increases.

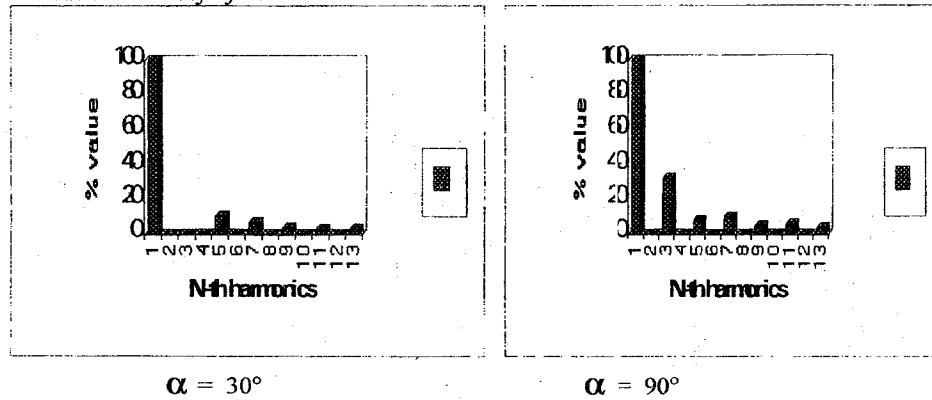


Fig. 16 Spectrum analysis of supply current (first method)

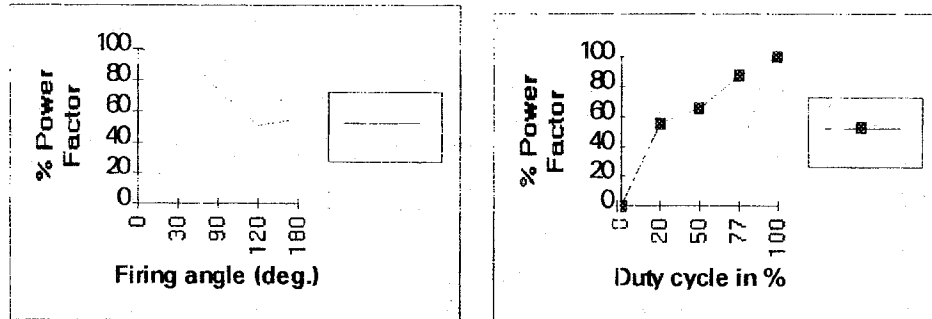


Fig. 15 Power factor against firing angle Fig.17 Power factor variation against duty cycle

4. Conclusion

A novel method of flux linkage between a single phase transformer windings control is used to control the load voltage. Two different strategies of flux control are presented . Phase control using triac or ac chopper topology with only one MOSFET. Employing such techniques reduces the supply current harmonics, improves the power factor at the supply terminals and smooth regulation of the load voltage. A computer program has been constructed for solving the system equations in different modes of operation , using

numerical techniques. A comparison reveals a good agreement between the theoretical and experimental results for the studied systems.

5. Symbols

V_s, i_s : supply voltage and current respectively.

R_L : load resistance .

R_p and R_s : transformer primary and secondary winding resistances respectively .

$\lambda_{12}, \lambda_{21}$: mutual flux linkage .

i_{Ls} : secondary current.

L_s : transformer secondary winding leakage inductance .

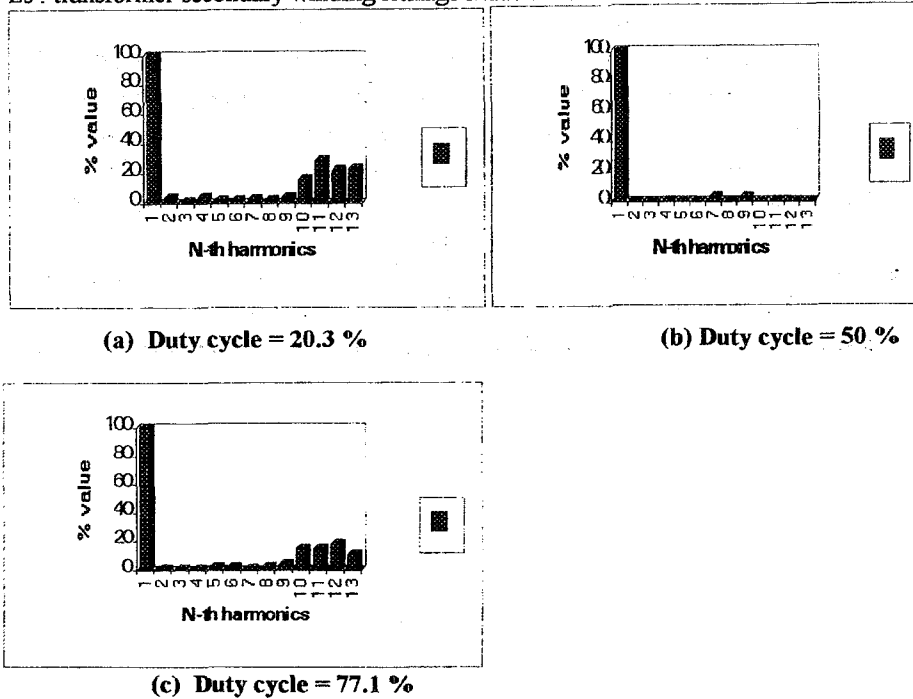


Fig. 18 Spectrum analysis of load voltage in different duty cycle values

6. References

- 1- M.S.Metwally, et al., "A new single phase ac controller for resistive loads", IEEE Trans. on IECI, vol. 24, No.3 , pp.277-281, 1977.
- 2-A.S.Abdel-Karim., "The moving -coil regulator a simplified treatment", Elect. machines and power systems, vol. 8, No.4, pp.395-402, 1983.
- 3- A.E Lashine et al., "Dynamic behavior of iron-cored coupled circuits", Eng. research bullet in faculty of Eng. & Tech., Menoufia Univ., vol.5, part II, 61-75, 1993.
- 4- Awad EL-Sabbe " series controlled inductance for supply quality improvement ". MEPCON' 97, Aix. Egypt, pp.487-492, 1997.
- 5- Do-Hyun Jang , et al. , " Improvement of input power factor in ac chopper using asymmetrical PWM technique " , IEEE trans.on industrial electronics, vol.42, No.2, 1995.
6. Khaled.EL-ADDOWEESH, and Adel L. MOHAMADEIN, "Microprocessor based harmonic elimination in chopper type ac voltage regulators", IEEE trans.on industrial electronics, vol.5, no.2, pp.179-185, April 1990.
7. A.M.Makky and A.A. Ibrahim, "a novel single-phase transformer circuit with inherent frequency and voltage changers", MEPCON'97, Alexandria, Egypt, Jan.4-6, pp. 209-213, 1997.
8. M.S.khanniche and I.D.W.Lake, "real time hysteresis controller for relay testing", IEE Proc., Electr. Power Appl., vol. 141, No.2, pp.71-76, March 1994.

بسم الله الرحمن الرحيم
حاكم جهد متغير حديث

د. عوض السيد عوض السبع
د. أشرف صلاح الدين زين الدين
قسم الهندسة الكهربائية - كلية الهندسة بشيبن الكوم

يقدم البحث حاكم جهد متغير أحادي الوجه حديث لحمل اما ان يكون مقاومة أو حمل حتى أو محرك أحادي الوجه باستخدام طريقتين مختلفتين . ففي الطريق الأولى يتم تغيير جهد الحمل بالتحكم في فيض التشابك بين ملفين لدائرة مغناطيسية . احد الملفين موصل بالتوالي مع الحمل والمنبع - الملف الآخر موصل معه زوج ثيرستور يتم التحكم في زاوية أشغالها بواسطة دائرة مصممة لذلك .
في الطريقة الثانية يتغير جهد الحمل بتغير فترات اشعال ترانزستور MOSFET موصل بأطراف الملف الثانى بدلا من الثيرستور حيث يتم تغيير فترات الأشغال باستخدام ميكروبروسور موصل مع الترانزستور في كل من الطريقتين تم عمل النموذج الرياضى وتحليله مع مقارنة النتائج النظرية والعملية ووجد توافق كبير بين العملى والنظرى .
يتميز حاكم الجهد المقترح ببساطته وقلة مركبات للتوافقيات في تيار المنبع لاستمرار تواجد هذا التيار على طول مدى التحكم مما يؤدي الى تحسين معامل القدرة عند المنبع بالمقارنة لحاكامات الجهد الأخرى . وعند تشغيل حاكم الجهد المقترح مع حمل حتى او مع محرك كهربي أعطى نتائج جيدة للتحكم في جهد الحمل .